Published November 18, 2002

JCB Article

Recombinant expression of the voltage-dependent anion channel enhances the transfer of Ca^{2+} microdomains to mitochondria

Elena Rapizzi,[1,2] Paolo Pinton,[1] György Szabadkai,[1] Mariusz R. Wieckowski,[1] Grégoire Vandecasteele,[1] Geoff Baird,[3] Richard A. Tuft,[2] Kevin E. Fogarty,[2] and Rosario Rizzuto[1]

[1]Department of Experimental and Diagnostic Medicine, Section of General Pathology, Telethon Center for Cell Imaging and Interdisciplinary Center for the Study of Inflammation, University of Ferrara, Via Borsari 46, I-44100 Ferrara, Italy
[2]Biomedical Imaging Group, University of Massachusetts Medical School, Worcester, MA 01655
[3]Howard Hughes Medical Institute and Department of Pharmacology, University of California, San Diego, CA 92093

Although the physiological relevance of mitochondrial Ca^{2+} homeostasis is widely accepted, no information is yet available on the molecular identity of the proteins involved in this process. Here we analyzed the role of the voltage-dependent anion channel (VDAC) of the outer mitochondrial membrane in the transmission of Ca^{2+} signals between the ER and mitochondria by measuring cytosolic and organelle $[Ca^{2+}]$ with targeted aequorins and Ca^{2+}-sensitive GFPs. In HeLa cells and skeletal myotubes, the transient expression of VDAC enhanced the amplitude of the agonist-dependent increases in mitochondrial matrix Ca^{2+} concentration by allowing the fast diffusion of Ca^{2+} from ER release sites to the inner mitochondrial membrane. Indeed, high speed imaging of mitochondrial and cytosolic $[Ca^{2+}]$ changes showed that the delay between the rises occurring in the two compartments is significantly shorter in VDAC-overexpressing cells. As to the functional consequences, VDAC-overexpressing cells are more susceptible to ceramide-induced cell death, thus confirming that mitochondrial Ca^{2+} uptake plays a key role in the process of apoptosis. These results reveal a novel function for the widely expressed VDAC channel, identifying it as a molecular component of the routes for Ca^{2+} transport across the mitochondrial membranes.

Introduction

The past years have witnessed a renewed interest in the role of mitochondria in calcium signaling (for reviews see Duchen, 2000; Rizzuto et al., 2000). Indeed, the direct measurement of Ca^{2+} with targeted recombinant probes or fluorescent indicators has demonstrated that in virtually all cell types a large rise in the Ca^{2+} concentration of the mitochondrial matrix ($[Ca^{2+}]_m$) parallels the cytoplasmic Ca^{2+} signals elicited by extracellular agonists (Rizzuto et al., 1993; Hajnoczky et al., 1995; Babcock et al., 1997; Montero et al., 2000). The apparent discrepancy between the amplitude of the cytosolic rises, and the low affinity of the mitochondrial uptake systems was reconciled by the demonstration that upon agonist-dependent Ca^{2+} release mitochondria are exposed to microdomains of $[Ca^{2+}]$ largely exceeding the $[Ca^{2+}]$ measured in the bulk cytoplasm (Rizzuto et al., 1998; Csordas et al., 1999). As to the physiological significance of mitochondrial Ca^{2+} homeostasis, numerous roles have emerged. On one hand, an increase in $[Ca^{2+}]_m$ can increase the production of ATP by activating matrix dehydrogenases in agonist-stimulated cells (McCormack et al., 1990; Robb-Gaspers et al., 1998; Jouaville et al., 1999). On the other hand, mitochondria can act as fixed buffers that either block the diffusion of the $[Ca^{2+}]_c$ rise in polarized cells (Tinel et al., 1999) or clear the $[Ca^{2+}]$ microdomain at the mouth of inositol 1,4,5-trisphosphate (IP_3)*-sensitive channels, thus shaping the kinetics of Ca^{2+} release from the ER (Landolfi et al., 1998; Boitier et al., 1999; Hajnoczky et al., 1999).

Despite the wide acceptance of the phenomenon of localized Ca^{2+} signaling between the ER and mitochondria, no molecular information is yet available on this important topic, since neither the mitochondrial Ca^{2+} transporters nor the structural proteins involved in the formation of the close

Address correspondence to Rosario Rizzuto, Dept. Exp. Diagn. Med. Sect. Gen. Pathol., Via Borsari 46, I-44100 Ferrara, Italy. Tel.: 39-0532-291361. Fax: 39-0532-247278. E-mail: r.rizzuto@unife.it

Key words: organelle; calcium; apoptosis; signal transduction; porin

*Abbreviations used in this paper: IP_3, inositol 1,4,5-trisphosphate; SERCA, sarco/endoplasmic reticulum Ca^{2+} ATPase; tBuBHQ, 2,5-di-(*tert*-butyl)-1,4-benzohydroquinone; VDAC, voltage-dependent anion channel.

Published November 18, 2002

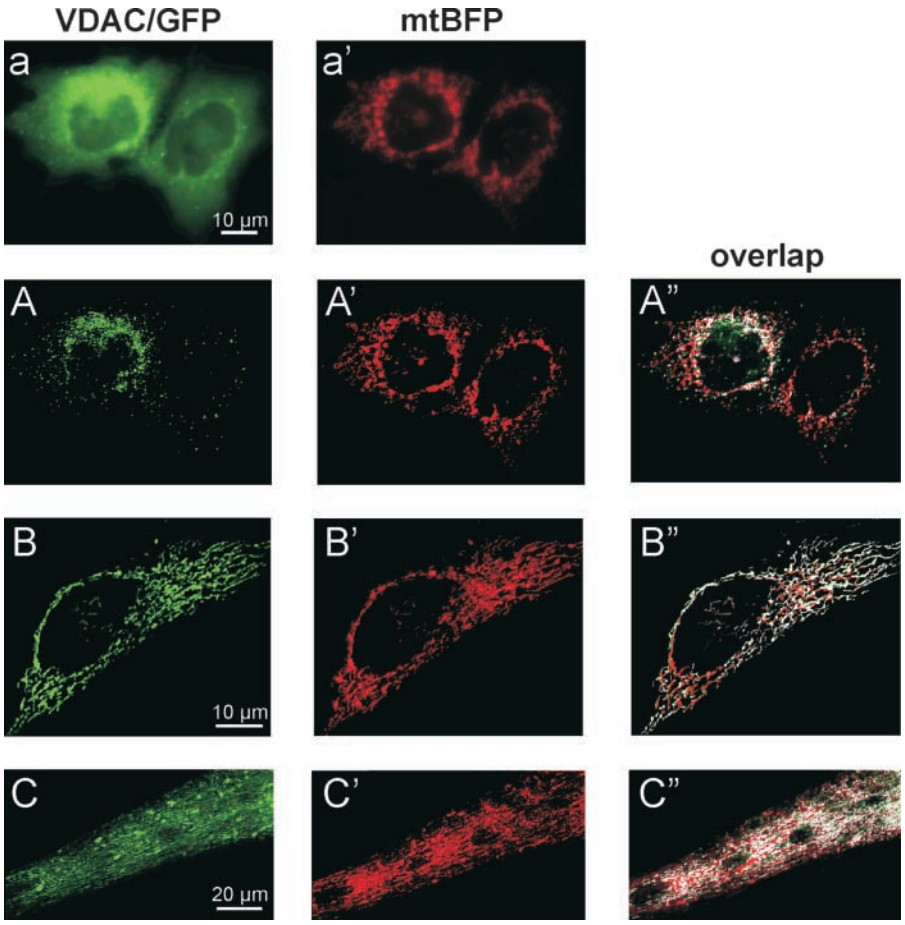

Figure 1. **Intracellular distribution of recombinantly expressed VDAC–GFP.** HeLa cells and primary myotubes were transfected with VDAC–GFP and placed on the stage of a fluorescence microscope. Acquired images (an example of raw images is shown in a and a′) were computationally deblurred as described in Materials and methods. A and B show the two different fluorescence patterns observed in VDAC-overexpressing HeLa cells (see Results); C shows the localization of VDAC–GFP in myotubes. The typical rod-like morphology of mitochondria is apparent from the mtBFP images in HeLa cells (A′ and B′) and myotubes (C′). A″, B″, and C″ represent the overlap images.

contacts between the two organelles have been identified. In this work, we have investigated the role of the voltage-dependent anion channel (VDAC) (Colombini, 1979; Mannella, 1998) of the outer mitochondrial membrane in modulating the Ca^{2+} response of the organelle. For this purpose, we have expressed a recombinant VDAC–GFP fusion protein and analyzed Ca^{2+} homeostasis at the subcellular level with recombinant Ca^{2+}-sensitive probes. By this means, we observed that VDAC is a key determinant of Ca^{2+} permeability at the ER–mitochondria contacts and thus is responsible for exposing the uptake systems of the inner mitochondrial membrane to the large [Ca^{2+}] gradients needed for rapidly accumulating Ca^{2+} in the organelle upon cell stimulation.

Results

Expression and subcellular localization of recombinant VDAC

In a first series of experiments, the expression and intracellular distribution of recombinant VDAC were tested. HeLa cells and primary cultures of rat skeletal myotubes were transfected with a GFP-tagged version of the rat VDAC1 cDNA (VDAC–GFP) and analyzed by digital imaging microscopy. In HeLa cells, most frequently we observed a pattern of widely diffused staining with punctate accumulations (Fig. 1 A). This appearance, which confirmed previous reports of VDAC expression (Sampson et al., 1998), was also typical of other cell lines, such as L929 and ECV cells (unpublished data). A second pattern (Fig. 1 B), showing a better sorting and incorporation in the outer mitochondrial membrane, was more rarely observed (in ~3% of VDAC-overexpressing cells). Conversely, in myotubes the visualization of VDAC–GFP always revealed the typical rod-like morphology of mitochondria (Fig. 1 C). In each case, mitochondrial localization was confirmed by cotransfection of VDAC–GFP with a blue GFP mutant targeted to the mitochondrial matrix (mtBFP) (Rizzuto et al., 1998). By alternating the excitation and emission wavelengths, the fluorescence images of the two GFP chimeras were obtained. The raw data were deconvolved as described in Materials and methods (an example is shown in Fig. 1, a and a′). The resulting images of VDAC–GFP (Fig. 1, A–C) and mtBFP (Fig. 1, A′–C′) were overlapped (Fig. 1, A′′–C′′), and the percentage of colocalization was calculated (see Materials and methods). In HeLa cells showing the distribution pattern of Fig. 1 A, 39 ± 4% of VDAC–GFP colocalized with mitochondria, whereas in HeLa cells showing the distribution pattern of Fig. 1 B the colocalization of VDAC–GFP with mitochondria was 57 ± 7%. In myotubes (Fig. 1 C), the colocalization was 55 ± 2% ($n = 5$ for each condition).

In parallel, we investigated the distribution of endogenous and transfected VDAC by subcellular fractionation and Western blot analysis using a polyclonal antibody recognizing both human and rat VDAC. Endogenous VDAC was detected only in the mitochondrial fraction (Fig. 2 A). Conversely, ~50% of transfected VDAC was detected in the mi-

Published November 18, 2002

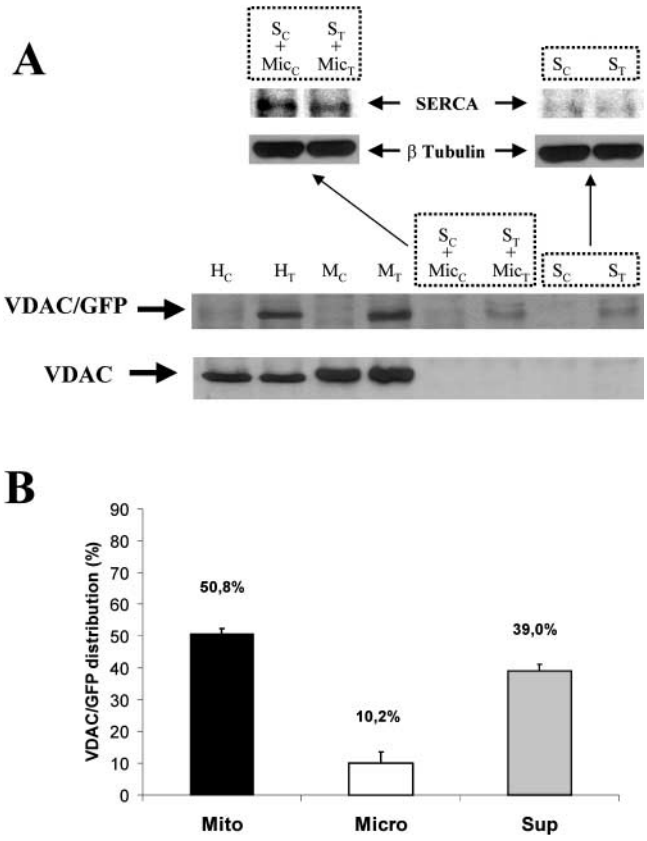

Figure 2. **Intracellular distribution of recombinantly expressed VDAC–GFP in HeLa cells.** (A) Endogenous VDAC and VDAC–GFP localization was evaluated by subcellular fractionation followed by immunoblotting. In the insets, the immunoblots of a cytosolic (β-tubulin) and ER (SERCA) protein are also shown for validating the separation of microsomal and cytosolic fractions by filtration (see Materials and methods). Total homogenates (H; 10 μg/lane), mitochondria (M; 10 μg/lane), supernatant with microsomes (S + Mic; 20 μg/lane), and pure supernatant (S; 20 μg/lane) from control (C) and VDAC–GFP-transfected (T) cells were separated on 14% SDS-PAGE and probed with an anti-VDAC polyclonal antibody as described in Materials and methods. The results shown are representatives of three replicates. (B) The graph shows the cellular distribution of overexpressed VDAC–GFP in HeLa cells calculated from the densitometric analysis of immunoblots ($n = 3$).

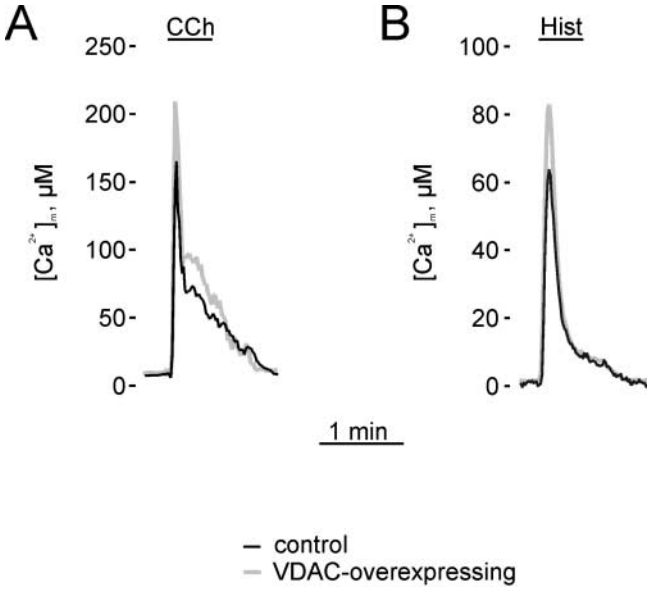

Figure 3. **Effect of VDAC overexpression on mitochondrial Ca^{2+} homeostasis in myotubes and HeLa cells.** $[Ca^{2+}]_m$ was measured in VDAC–GFP + mtAEQmut (VDAC-overexpressing cells, gray traces) or mtAEQmut (control, black traces)-expressing cells. Where indicated, myotubes (A) and HeLa cells (B) were stimulated with 500 μM carbachol and 100 μM histamine, respectively, added to the perfusion medium. The traces are representative of >10 trials.

tochondrial fraction, ~10% in microsomes, and ~40% in the soluble supernatant (Fig. 2, A and B) in good agreement with the mtBFP and VDAC–GFP colocalization data. The Western blot also allowed us to obtain a rough estimate of the extent of VDAC overexpression by comparing the signals of endogenous and transfected VDAC that appear in an ~3:1 ratio, respectively. Considering an efficiency of transfection of 30–40%, it can be estimated that in transfected cells recombinant VDAC is expressed at a level comparable to that of the endogenous counterpart.

The effect of VDAC overexpression on mitochondrial Ca^{2+} responses

We then investigated the effect of VDAC overexpression on mitochondrial Ca^{2+} homeostasis using a specifically targeted chimera of the Ca^{2+}-sensitive photoprotein aequorin, mtAEQmut (Montero et al., 2000). A first series of experiments was performed in skeletal myotubes. Myoblasts were transfected with either VDAC–GFP and mtAEQmut (VDAC overexpressing) or with mtAEQmut (control) and analyzed 7 d after transfection, i.e., when expression of the transgene is limited to myotubes (Brini et al., 1997). After aequorin reconstitution, the coverslips with the cells were transferred to the luminometer chamber and recording was started. Where indicated, myotubes were challenged with 500 μM carbachol. The stimulation of nicotinic receptors induces depolarization of the plasma membrane followed by both Ca^{2+} entry via voltage-operated Ca^{2+} channels and Ca^{2+} release from the sarcoplasmic reticulum. As a consequence, a major $[Ca^{2+}]$ rise was elicited in the cytoplasm that caused a large and rapid Ca^{2+} uptake into the mitochondrial matrix as described previously (Brini et al., 1997). This $[Ca^{2+}]_m$ rise was markedly larger in VDAC-overexpressing cells (207 ± 7 μM versus 160 ± 4 μM in control cells, $n = 20$, $P < 0.001$) (Fig. 3 A).

Then, we analyzed $[Ca^{2+}]_m$ responses in HeLa cells. In the experiment of Fig. 3 B, VDAC-overexpressing and control HeLa cells were challenged with histamine, which causes generation of IP_3 and thus the release of Ca^{2+} from the ER. As for myotubes, the $[Ca^{2+}]_m$ peak was markedly larger in VDAC-overexpressing HeLa cells than in controls (85 ± 3 μM versus 62 ± 2 μM, respectively, $n = 21$, $P < 0.001$). As the effect of VDAC overexpression on $[Ca^{2+}]_m$ was clear both in myotubes and HeLa cells, further characterization was performed in the simpler HeLa cell model.

The effect of VDAC overexpression on ER Ca^{2+} handling

We then tested whether the enhancement of mitochondrial Ca^{2+} uptake could be explained by an effect on the state of

Published November 18, 2002

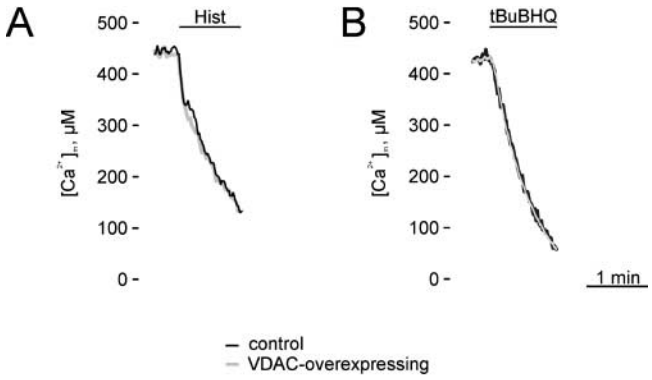

Figure 4. **Effect of VDAC overexpression on ER Ca^{2+} homeostasis.** $[Ca^{2+}]_{er}$ was measured with erAEQmut. Where indicated, the cells were challenged with 100 μM histamine (A) or 30 μM tBuBHQ (B). The traces are representative of >10 trials. VDAC-overexpressing and control cells are labeled as in Fig. 3.

filling of the intracellular Ca^{2+} stores and/or the kinetics of Ca^{2+} release, i.e., whether the effect on mitochondria is secondary to a global alteration in Ca^{2+} signaling. For this purpose, the $[Ca^{2+}]$ of the ER lumen ($[Ca^{2+}]_{er}$) was measured with a specifically targeted aequorin chimera (erAEQmut) (Barrero et al., 1997) (Fig. 4). No significant difference could be appreciated between VDAC-overexpressing and control cells in the steady state $[Ca^{2+}]_{er}$ (480 ± 32 μM in VDAC-overexpressing cells versus 472 ± 33 μM in controls, $n = 20$, $P > 0.05$), indicating that VDAC does not affect the state of filling of the Ca^{2+} stores. Upon stimulation with histamine, a rapid drop in $[Ca^{2+}]_{er}$ was observed followed by a slower virtually complete release of stored Ca^{2+} (Fig. 4 A). The kinetics and amplitude of $[Ca^{2+}]_{er}$ decrease were very similar in VDAC-overexpressing and control cells, indicating that the effect of VDAC on mitochondrial Ca^{2+} homeostasis does not depend on the modification of ER Ca^{2+} storage or release. Given that a minor fraction (~10%) of transfected VDAC was detected in the microsomal fraction (thus also in the ER), we decided to directly demonstrate that it does not increase the Ca^{2+} leak from the ER (thus supporting the indirect evidence provided by the lack of effect on the steady state $[Ca^{2+}]_{er}$). For this purpose, we evaluated the rate of Ca^{2+} discharge from the ER upon inhibition of the sarco/endoplasmic reticulum Ca^{2+} ATPase (SERCA) in VDAC-overexpressing and control cells (Fig. 4 B). Where indicated, the cells were treated with the SERCA blocker 2,5-di-(*tert*-butyl)-1,4-benzohydroquinone (tBuBHQ; 30 μM). This caused rapid emptying of ER Ca^{2+} with no difference in kinetics and amplitude between VDAC-overexpressing and control cells.

The effect of VDAC overexpression on mitochondrial Ca^{2+} uptake in permeabilized cells

Since no significant difference between VDAC-overexpressing and control HeLa cells was measured in the ER Ca^{2+} handling, the simplest explanation for the previous results would be that VDAC increases the efficiency of mitochondria in accumulating Ca^{2+}, e.g., that it directly stimulates Ca^{2+} uptake. If this is the case, a faster rate of mitochondrial Ca^{2+} uptake should be directly measured in permeabilized

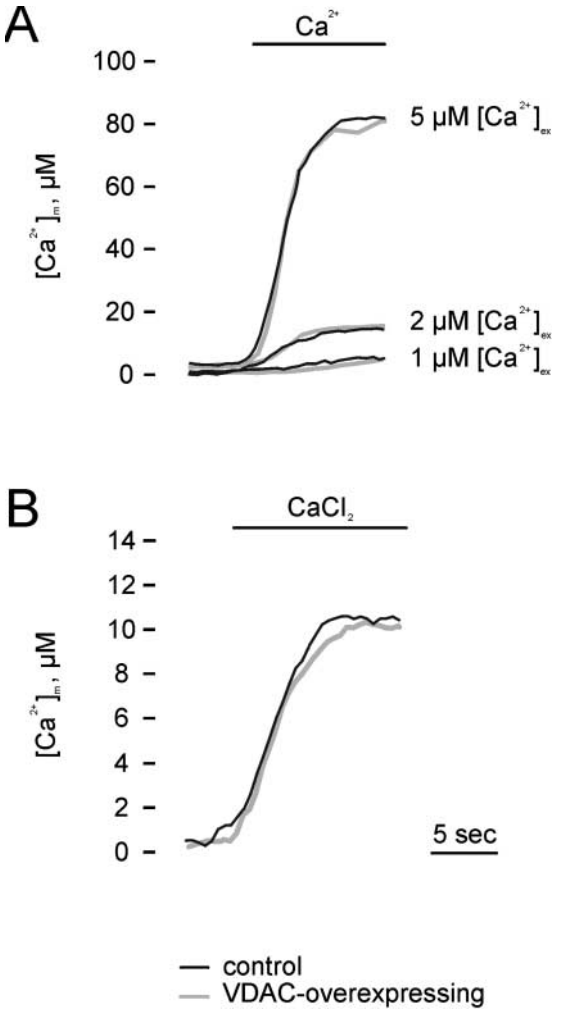

Figure 5. **Effect of VDAC overexpression on mitochondrial Ca^{2+} uptake in permeabilized HeLa cells and during capacitative Ca^{2+} entry in intact HeLa cells.** In A, cells were permeabilized as described in Materials and methods. Where indicated, IB/EGTA was replaced with Ca^{2+}-buffered IB containing 1, 2, and 5 μM $[Ca^{2+}]$. In B, capacitative Ca^{2+} entry was initiated in intact tBuBHQ-treated cells by replacing KRB/EGTA with KRB supplemented with 2 mM $CaCl_2$. Trace labeling and all conditions as in Fig. 3.

cells perfused with defined $[Ca^{2+}]$. Fig. 5 A shows representative traces of mitochondrial Ca^{2+} accumulation in permeabilized control and VDAC-overexpressing HeLa cells. The three sets of traces correspond to $[Ca^{2+}]$ in the perfusion medium of 1, 2, and 5 μM. At any $[Ca^{2+}]$ used, no significant difference could be detected in the rate of mitochondrial Ca^{2+} uptake between the two groups of cells (1.4 ± 0.5 μM/s versus 1.0 ± 0.03 μM/s for 1 μM $[Ca^{2+}]_{ex}$, 10 ± 2 μM/s versus 10 ± 3 μM/s for 2 μM $[Ca^{2+}]_{ex}$, 21 ± 3 μM/s versus 19 ± 1 μM/s for 5 μM $[Ca^{2+}]_{ex}$, $n = 9$ and $P > 0.05$ for each condition data).

Further support to the notion that VDAC overexpression does not generally increase mitochondrial Ca^{2+} uptake was obtained also in intact cells by investigating the Ca^{2+} rise elicited exclusively by capacitative Ca^{2+} entry. In these experiments, cells were treated with tBuBHQ (50 μM) for 2 min to completely deplete the Ca^{2+} stores, then Ca^{2+} entry

Published November 18, 2002

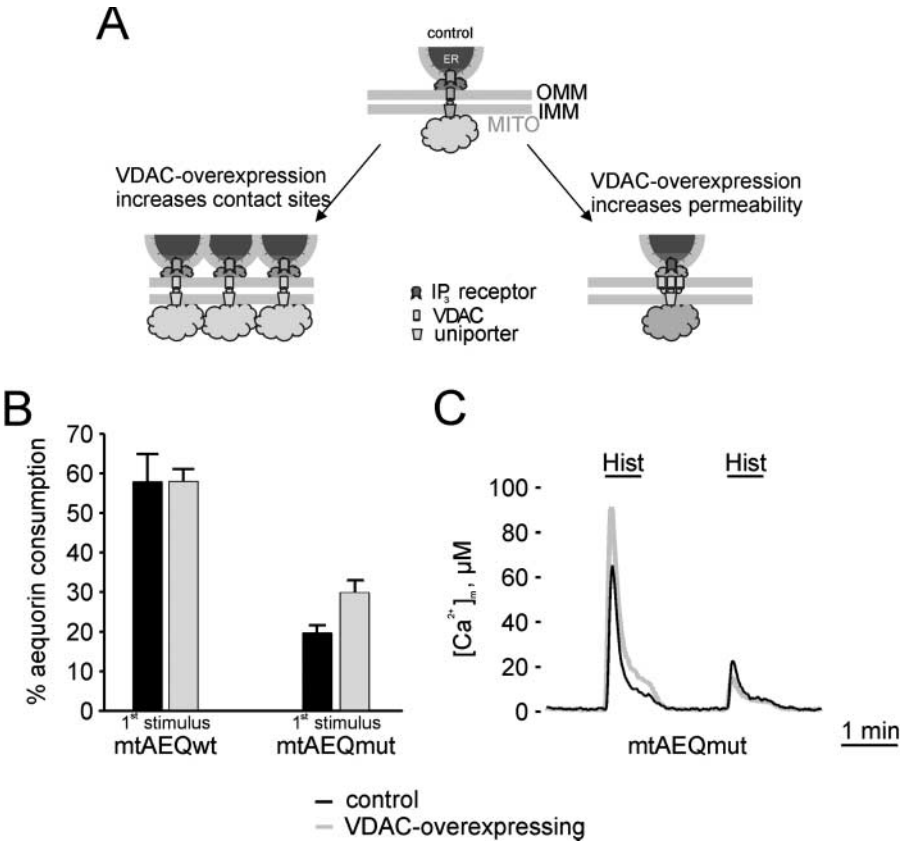

Figure 6. **Schematic model of the alternative mechanisms by which VDAC overexpression could affect mitochondrial Ca^{2+} homeostasis and effect of VDAC overexpression on mitochondrial Ca^{2+} uptake in repetitively challenged HeLa cells.** (A) A higher number of VDAC molecules could either induce the formation of additional ER/mitochondria "signaling units" (left) or increase the outer membrane permeability at the contacts between mitochondria and ER (right). (B) Aequorin consumption in the 1st agonist-dependent increases in $[Ca^{2+}]_m$ using high and low affinity mitochondrial-targeted aequorin (mtAEQwt, mtAEQmut) in control and VDAC-overexpressing cells (black and gray columns, respectively). The data show the integral of aequorin light emission during the $[Ca^{2+}]_m$ increase, expressed as the percentage of the total light discharge of the experiment. (C) Representative traces of the increases in $[Ca^{2+}]_m$ caused by repetitive histamine stimulation as measured with mtAEQmut. Trace labeling and all conditions as in Fig. 3.

was initiated by switching the medium from Ca^{2+}-free Krebs-Ringer modified buffer (KRB) to KRB supplemented with 2 mM $CaCl_2$ (in the continuous presence of tBuBHQ). This maneuver caused an increase in both $[Ca^{2+}]_c$ (unpublished data) and $[Ca^{2+}]_m$ with no difference in Ca^{2+} uptake between VDAC-overexpressing and control cells (peak, 11 ± 1 μM versus 11 ± 1 μM; rates, 5 ± 1 μM/s versus 5 ± 1 μM/s, respectively, $n = 12$, $P > 0.05$) (Fig. 5 B). Therefore, it must be concluded that a difference in mitochondrial Ca^{2+} uptake between VDAC-overexpressing and control cells can be seen only upon agonist-stimulated (IP_3-mediated) release of Ca^{2+} from the ER, and VDAC has no direct effect on mitochondrial Ca^{2+} uptake.

VDAC increases the Ca^{2+} permeability of ER–mitochondria contact sites

The two remaining explanations for the effects of VDAC are that either it generates an increase of outer membrane permeability at the ER–mitochondria contacts, or, alternatively, it regulates the formation of the contacts themselves. To discriminate between these possibilities (schematically shown in Fig. 6 A), we took advantage of an inherent property of aequorin, i.e., its irreversible reaction and thus progressive consumption during the experiment.

We used the wild-type high affinity mtAEQ chimera (mtAEQwt) that is completely discharged in the highly responding areas of the mitochondrial network (Montero et al., 2000). Thus, it is not suitable for the exact assessment of the $[Ca^{2+}]$ in these regions, but the fraction of the probe consumed during the stimulation can be used as an index of the extension of highly responding areas of the network that are presumably involved in the ER–mitochondrial interaction. Consequently, when the cells are repetitively stimulated with an agonist the first stimulation consumes a large fraction of the probe (~60%) (Fig. 6 B), whereas a much smaller fraction is consumed in the 2nd and 3rd pulse (~11 and 5%, respectively [unpublished data]). If the number of ER–mitochondria contacts were increased in VDAC-overexpressing cells, a larger portion of mitochondria should consume their aequorin pool during the first stimulation. This is not the case (Fig. 6 B), indicating that VDAC increases the efficacy of the existing contacts (thus enhancing the $[Ca^{2+}]_m$ rise in the highly responding domains), an effect that cannot be detected by mtAEQwt that is already fully discharged in these regions even in control cells. Conversely, a low affinity mutant (mtAEQmut) is only partially consumed in the highly responsive mitochondrial regions, and thus a larger fraction of the probe is consumed in VDAC-overexpressing cells (Fig. 6 B). Under those circumstances, it can be expected that in a subsequent agonist stimulation mtAEQmut reveals a paradoxical larger $[Ca^{2+}]_m$ rise in control cells, simply reflecting the fact that more functional mtAEQmut remains present in the highly responding domains after the first stimulation. This is clearly apparent in the experiment of Fig. 6 C in which mtAEQmut-expressing HeLa cells were challenged with two consecutive histamine pulses. In the second agonist challenge, the $[Ca^{2+}]_m$ peak is apparently smaller in VDAC-overexpressing than in control cells (18 ± 2 μM versus 21 ± 2 μM, $n = 7$, $P > 0.05$), reflecting the larger aequorin consumption (30 ± 2% versus 20 ± 1%, $n = 7$, $P < 0.05$) occurring in VDAC-overexpressing cells during the first stimulation (Fig. 6 B).

Published November 18, 2002

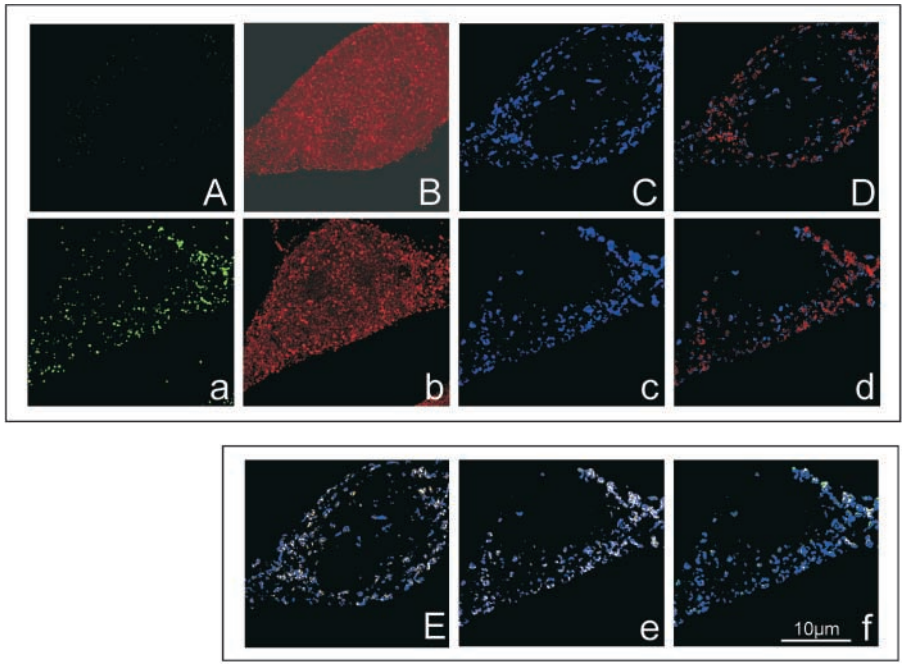

Figure 7. **Spatial relationship between ER, VDAC, and mitochondria.** Representative images of control and VDAC-overexpressing cells (upper and lowercase letters, respectively, $n = 5$) are shown. Images were acquired, deblurred, thresholded, and analyzed as described in Materials and methods. VDAC–GFP (VDAC overexpressed in the transfected cells, no signal in the control cell) (A and a); anticalreticulin labeling (B and b); mtBFP (C and c); three-dimensional overlay between mtBFP and anticalreticulin and in both images the percentage of mitochondrial surface that colocalized with ER was ~29% (D and d). Panels E and e shows the overlays between mtBFP (blue), total mitochondrial endogenous VDAC (orange and white), and the mitochondrial endogenous VDAC that colocalized with calreticulin (white only), which is almost 63% of the total mitochondrial endogenous VDAC in both cases. Panel f shows the overlay between mtBFP (blue), total overexpressed mitochondrial VDAC–GFP (green and white), and mitochondrial VDAC–GFP that colocalized with calreticulin (white only).

To further investigate the spatial relationship between ER and mitochondria, we used the immunocytochemistry approach. Briefly, we transfected HeLa cells with mtBFP or mtBFP + VDAC–GFP (control and VDAC-overexpressing, respectively), fixed the samples, incubated them with an anticalreticulin (a typical ER marker) antibody, and then treated the cells with a secondary antibody conjugated with Cy5. In doing so, we were able to image the cells with three different wavelengths simultaneously (see Materials and methods). The resulting images were deconvolved and overlapped (Fig. 7, A–D and a–d). We then calculated the percentage of mitochondrial surface (mtBFP) that colocalized with calreticulin (Cy5) (see Materials and methods). In both the conditions (control and VDAC-overexpressing cells), the average colocalization was ~29% (control, 33 ± 13% $n = 3$ and VDAC-overexpressing cells, 25 ± 13%, $n = 4$, $P > 0.05$), suggesting that at least in our experimental condition the presence of VDAC did not increase the number of close contacts between ER and mitochondria. Similar results were obtained using an anti-SERCA 2 antibody to label the ER (unpublished data). We also checked the relationship between mitochondria and Golgi apparatus in control and VDAC-overexpressing cells using an anti–human golgin-97 to label the organelle. The average colocalization of mitochondrial surface with the Golgi was ~0.4% (control, 0.4 ± 0.2% and VDAC-overexpressing cells, 0.4 ± 0.3%, $n = 6$, $P > 0.05$), indicating that also the spatial arrangement between Golgi and mitochondria was not altered by the overexpression of VDAC.

To investigate the spatial relationship of VDAC and contact sites with the ER, we performed a second series of experiments. Control and VDAC-overexpressing cells were treated with a anti–human VDAC monoclonal antibody (recognizing only endogenous VDAC) revealed by an Alexa 594–conjugated secondary antibody. We then statistically analyzed the colocalization (Moore et al., 1993) between (a) endogenous VDAC and calreticulin and (b) overexpressed VDAC and calreticulin. If the endogenous VDAC and calreticulin were in fact distributed independently of each other, then (according to Bayes Law) the probability of the two colocalizing would be equal to the product of the individual probabilities of VDAC and calreticulin being found at the mitochondrial surface. From the images, we were able to calculate (see Materials and methods) the percentage of mitochondrial surface voxels containing calreticulin (Fig. 7 D, d, red pixels), the percentage containing VDAC (Fig. 7 E, e, orange and white pixels), and the percentage containing both (colocalization of VDAC with calreticulin [Fig. 7 E, e, white pixels only]). We used the calculated percentages as estimates of these probabilities. The colocalization calculated from the images was 1.52 ± 0.13 times larger than that predicted assuming independence of VDAC and calreticulin. Thus, it appears that the VDAC and calreticulin were not independently distributed. The sites of colocalization were not homogeneously distributed (not present on the entire mitochondrial surface), suggesting that they were forming clusters both in the control and VDAC-overexpressing cells. In fact, the endogenous VDAC was spatially concentrated at the ER contact sites with ~63% of VDAC colocalizing with calreticulin (Fig. 7 E, e). There was no statistical difference between control and VDAC-overexpressing cells (57 ± 8% and 68 ± 5%, respectively, $n = 3$, $P > 0.05$). In VDAC–GFP-overexpressing cells, 32 ± 9% of the transfected VDAC is also present at the contact sites (Fig. 7 f), indicating partial clustering also of the recombinant protein. In summary, these results suggest that the overexpression of VDAC does not alter the spatial arrangement of contact sites between the ER and mitochondria and that endogenous

Published November 18, 2002

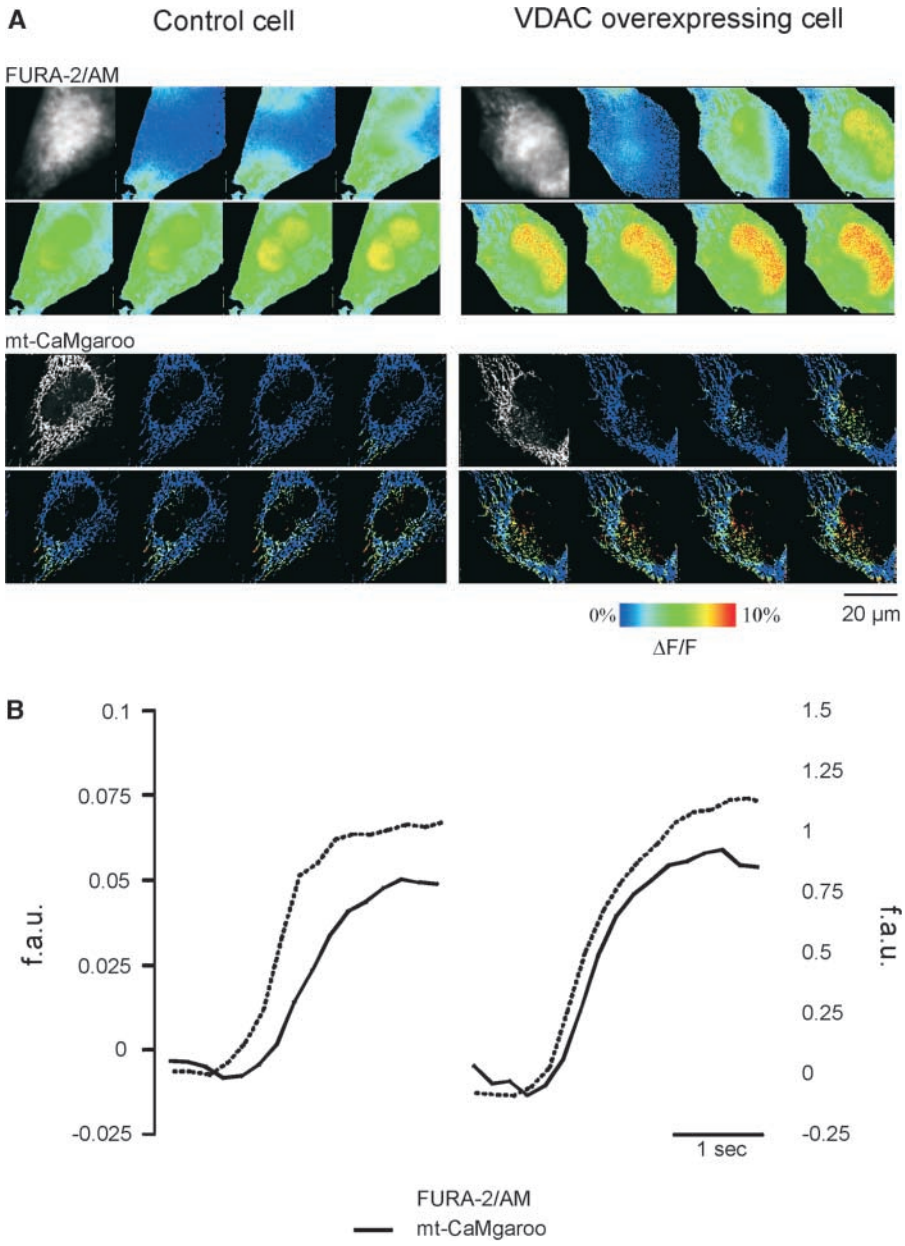

Figure 8. **Simultaneous single cell imaging of mitochondrial and cytosolic $[Ca^{2+}]$ changes in single cell.** In A, the imaging of Fura-2/AM (top) and mt-CaMgaroo (bottom) is shown. The black and white images show Fura-2/AM and three-dimensional CaMgaroo distribution within the cells. The pseudocolored images (350 nm/380 nm ratio for Fura-2/AM and 514 excitation for CaMgaroo) show the changes in fluorescence after a 5-s puff of histamine (10 μM). At each time point (200 ms apart), the $[Ca^{2+}]$ is measured simultaneously in the cytosol and mitochondria as described in Materials and methods. In B, the traces representing the changes in fluorescence (f.a.u., fluorescence arbitrary units) of $[Ca^{2+}]_c$ (dotted lines) and $[Ca^{2+}]_m$ (continuous lines) are shown. Images and traces are representative of six trials.

VDAC is clustered at these sites. Furthermore, overexpression leads to an increased presence of VDAC at these sites, further supporting the interpretation of the aequorin functional results.

High speed imaging of mitochondrial Ca^{2+} changes reveals a shorter delay of the mitochondrial Ca^{2+} response

To directly demonstrate the role of VDAC in allowing the diffusion of the Ca^{2+} microdomain from the mouth of the IP_3 receptor to the mitochondrial Ca^{2+} uniporter, we performed high speed single cell imaging of cytosolic and mitochondrial Ca^{2+} changes. For this purpose, HeLa cells were transfected with a mitochondrially targeted CaMgaroo (a Ca^{2+}-sensitive yellow variant of GFP) (Baird et al., 1999; Griesbeck et al., 2001) and loaded with Fura-2/AM and were analyzed with an imaging system based on a highly sensitive camera and fast alternation of excitation and emission wavelengths. As described in detail in Materials and methods, with this system a CaMgaroo image and a Fura-2/AM ratio image pair are acquired within 25 ms every 200 ms for 39.6 s. Fig. 8 shows the kinetics of $[Ca^{2+}]_c$ and $[Ca^{2+}]_m$ increase upon histamine stimulation in control and VDAC-overexpressing cells. It is apparent that the $[Ca^{2+}]_c$ rise is followed by a delayed (460 ± 98 ms, $n = 6$) upstroke of $[Ca^{2+}]_m$ as described previously (Drummond et al., 2000; Gerencser and Adam-Vizi, 2001). Interestingly, this delay is significantly ($P < 0.05$) shortened in VDAC-overexpressing cells (200 ± 49 ms, $n = 6$). Moreover, in VDAC-overexpressing cells the amplitude of the peak $[Ca^{2+}]_m$ rise is increased compared with controls ($\Delta F/F_0 = 0.063 \pm 0.005$ versus 0.047 ± 0.007, respectively, $n = 6$, $P < 0.05$) in good agreement with the results obtained with the aequorin probe.

Published November 18, 2002

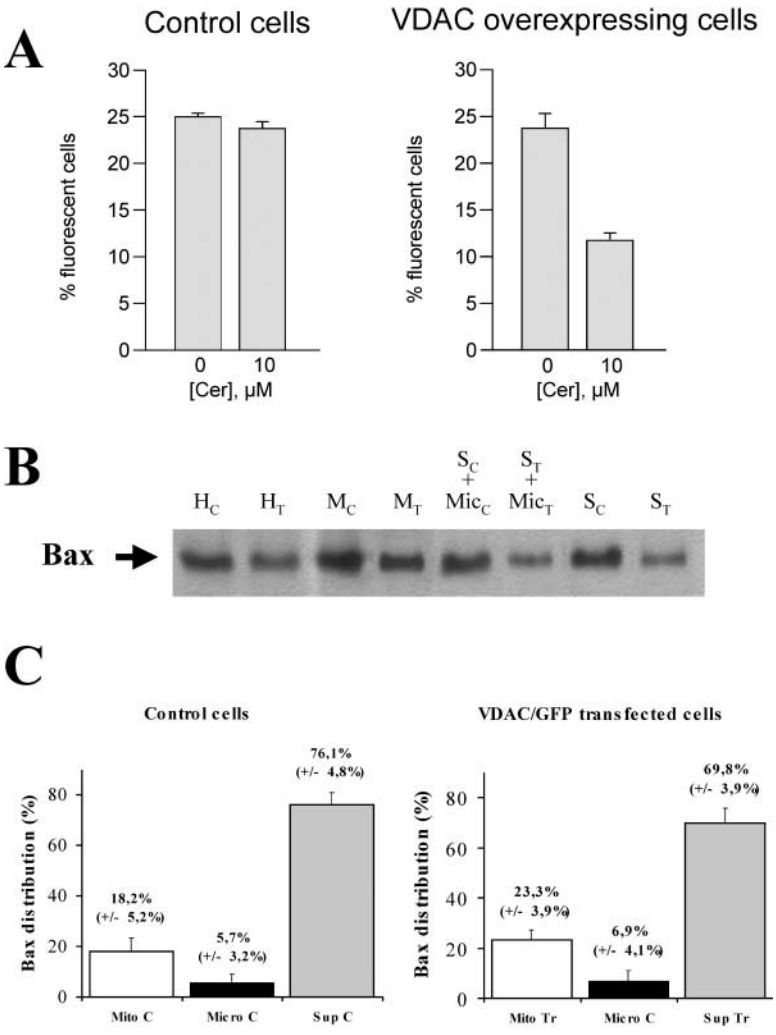

Figure 9. **C_2 ceramide-induced cell death and intracellular Bax localization.** (A) Cell viability was evaluated after a 16-h treatment with C_2 ceramide (10 μM) in control (mtGFP-transfected) and VDAC-overexpressing (VDAC–GFP-transfected) cells. The data show the percentage of GFP fluorescent cells in the surviving cell population (see Results). Average values were obtained from analyzing >50 fields in three independent experiments. (B) Effect of VDAC overexpression on intracellular Bax distribution in HeLa cells. Bax localization was evaluated by immunoblotting. Total homogenates (H; 10 μg/lane), mitochondria (M; 10 μg/lane), supernatant with microsomes (S + Mic; 10 μg/lane) and pure supernatant (S; 10 μg/lane) from control (C) and VDAC–GFP-transfected (T) cells were separated on 14% SDS-PAGE and probed with polyclonal antibodies against Bax as described in Materials and methods. The results shown are representatives of three replicates. (C) The graph shows the cellular distribution of Bax in HeLa cells calculated from the densitometric analysis of immunoblots ($n = 3$).

Overexpression of VDAC enhances the sensitivity of cells to the apoptotic stimulus ceramide

In a previous paper, we have shown that ceramide induces a sustained $[Ca^{2+}]_m$ rise that causes a major morphological alteration of mitochondria (Pinton et al., 2001). Given the effect of VDAC on mitochondrial Ca^{2+} uptake and the observation that VDAC is up-regulated in apoptosis-sensitive cells (see Discussion), we decided to investigate whether recombinant expression of VDAC enhances the susceptibility to apoptosis. For this purpose, HeLa cells were transfected with VDAC–GFP and treated with the apoptotic stimulus ceramide. The efficacy of the apoptotic stimulus was verified by microscopic count of fluorescent surviving cells as described previously (Pinton et al., 2001). Indeed, when the cells are transfected with a fluorescent probe with no effect on apoptosis (mtGFP, controls) ceramide is equally effective on transfected and nontransfected cells, and thus the percent of fluorescent cells is the same before and after ceramide addition (25 ± 1% versus 24 ± 2%, $P > 0.05$) (Fig. 9 A). Conversely, when the cells are transfected with a protein-enhancing apoptosis (in this case VDAC) tagged with GFP transfected cells are more sensitive to apoptosis, and thus the percentage of fluorescent cells is lower after ceramide addition (24 ± 4% versus 12 ± 3%, $P < 0.05$) (Fig. 9 A).

We verified whether the proapoptotic effect could be due to up-regulation or selective recruitment of other effectors, such as proapoptotic members of the Bcl-2 family. We thus investigated by Western blotting the levels and subcellular distribution of Bax in VDAC-overexpressing and control cells. The results are shown in Fig. 9, B and C, respectively. It is apparent that in the VDAC-overexpressing cells there is neither up-regulation of Bax (rather, there is an ~30% reduction) nor any difference in its subcellular distribution (e.g., mitochondrial recruitment).

We then investigated whether the higher sensitivity to apoptosis can be attributed to the enhancement of mitochondrial Ca^{2+} uptake and the ensuing alteration of organelle morphology. To analyze mitochondrial morphology, HeLa cells were transfected with the fluorescent mitochondrial marker mtRFP and placed on the stage of the fluorescence microscope. Fig. 10 shows three images of control (mtRFP-transfected) and VDAC-overexpressing (VDAC–GFP- and mtRFP-cotransfected) cells acquired immediately before (time 0) and 30 and 60 min after the addition of the 10 μM ceramide. In both control and VDAC-overexpressing cells, the largely interconnected mitochondrial network can be recognized at time 0. In control cells, minimal changes can be appreciated after 30 min, which become more apparent

Published November 18, 2002

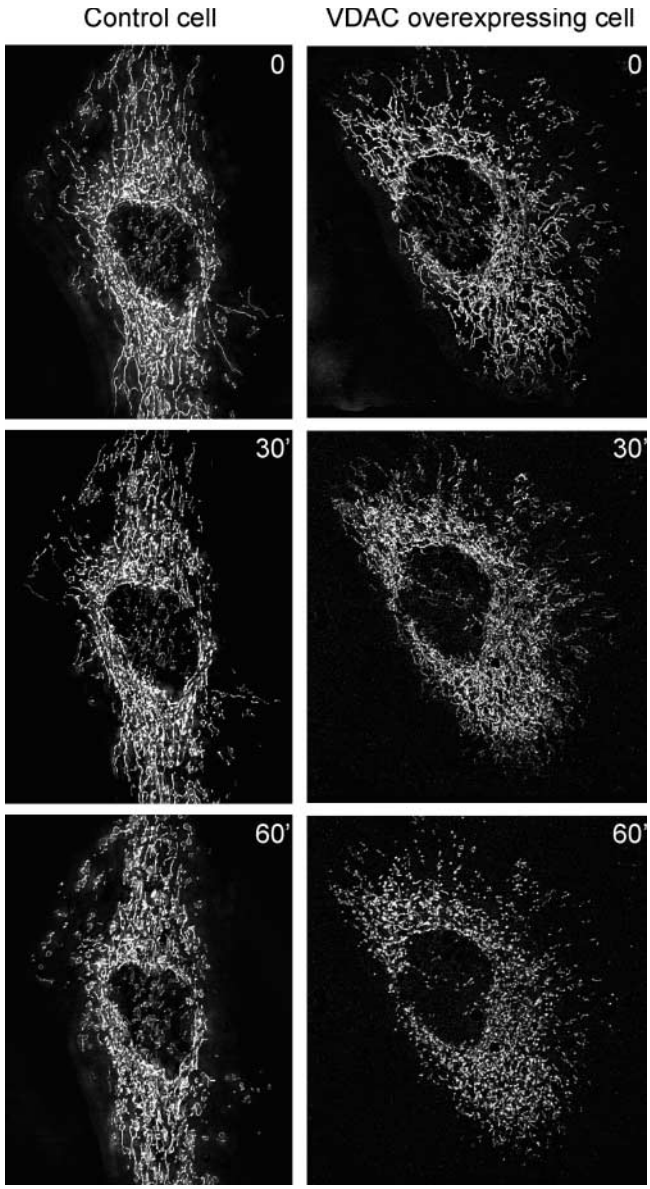

Figure 10. **Morphological changes in the mitochondrial network induced by C_2 ceramide.** Mitochondrial structure was evaluated in control (mtRFP-transfected) and VDAC-overexpressing (mtRFP-VDAC–GFP–cotransfected) cells immediately before (time 0) and 30 and 60 min after the addition of C_2 ceramide (10 μM). The images are representative of >10 independent experiments that gave similar results.

after 60 min (rounding and breaking of the network). In VDAC-overexpressing cells, mitochondrial alterations are obvious after 30 min, and a complete rupture of the three-dimensional network can be noticed after 60 min.

Discussion

Despite the renewed interest in the role of mitochondria in calcium signaling, the molecular mechanisms that allow these organelles to rapidly accumulate and release large Ca^{2+} loads are still completely obscure. In the search for the molecular determinants of mitochondrial Ca^{2+} responses, we focused on VDAC, the voltage-dependent anion channel of the outer mitochondrial membrane. VDAC is a large diameter (2.5–3 nm) channel that is permeable to ions and small molecules (cutoff 5,000 D) (Colombini, 1979; Mannella, 1998). Its state of opening has been proposed to be regulated by NADH and other effectors (Lee et al., 1996) and by the interaction with regulatory proteins, such as the members of the Bcl-2 protein family (Vander Heiden et al., 2001). More recently, VDAC has been shown to be highly permeable to Ca^{2+} and to contain binding sites for ruthenium red that inhibit channel opening (Gincel et al., 2001). VDAC may represent a key component of mitochondrial Ca^{2+} homeostatic mechanisms, potentiating Ca^{2+} responses by different mechanisms. First, by acting as a large conductance channel it could allow the rapid diffusion of Ca^{2+} across the outer mitochondrial membrane and thus allow the low affinity uniporter of the inner membrane to be exposed to the microdomains of high $[Ca^{2+}]$ generated by the opening of ER Ca^{2+} channels. Alternatively, also considering that VDAC has been proposed to be part of a larger complex including the adenine nucleotide transporter, cyclophilin D, the peripheral benzodiazepine receptor, and members of the Bcl-2 family (Crompton, 2000), it could interact with structural components of the ER and thus be part of the molecular machinery docking mitochondria to Ca^{2+} stores.

In this paper, we identified VDAC as a positive regulator of mitochondrial Ca^{2+} accumulation. This was the case in all the cell types investigated, from skeletal myotubes to stable cell lines such as HeLa, ECV, and L929 cells. This effect was not due to a generalized increase in the permeability of the outer membrane and/or an effect on the uptake systems of the inner membrane as deduced by (a) the measurement of mitochondrial Ca^{2+} uptake rates in permeabilized cells and (b) the lack of effect on the $[Ca^{2+}]_m$ rise elicited by Ca^{2+} entry through plasmamembrane channels. The possibility that VDAC is involved in the formation of new ER–mitochondria contacts is ruled out by the data obtained with high affinity aequorin, which reveals the highly responding domains of the mitochondrial network.

Overall, our results indicate that VDAC overexpression affects the Ca^{2+} permeability at the domains of the ER–mitochondria cross-talk. This was directly demonstrated by the direct double imaging of mitochondrial and cytosolic $[Ca^{2+}]$ changes using a targeted Ca^{2+}-sensitive GFP chimera and a fluorescent dye, respectively. This experiment confirms previous data, indicating a delay between the cytosolic and the mitochondrial Ca^{2+} rise (Drummond et al., 2000; Gerencser and Adam-Vizi, 2001) and shows that this delay is drastically shortened by VDAC overexpression. These data indicate that the transfer of the $[Ca^{2+}]$ microdomain generated at the mouth of the IP_3 receptors across the outer membrane that allows the low affinity uniporter of the inner membrane to be exposed to high $[Ca^{2+}]$ and thus rapidly accumulate Ca^{2+} in the matrix is critically dependent on the VDAC repertoire. Thus, the permeability of the outer membrane at the ER–mitochondria contacts is a kinetic bottleneck for the process of mitochondrial Ca^{2+} homeostasis. This could depend on various nonmutually exclusive possibilities: (a) the selective clustering of VDAC channels at the ER–mitochondria contact sites supported by immunofluorescence data of this paper and previous immunoelectron microscopy experiments that demonstrated the clustering of VDAC and ryan-

Published November 18, 2002

odine receptors at sarcoplasmic reticulum/mitochondria contacts (Shoshan-Barmatz et al., 1996), (b) a different state of opening in these domains (different states of opening of VDAC channels, responsible for differences in anion permeability, were described by Rostovtseva and Colombini [1996]), or (c) the strict dependence of a highly transient phenomenon, such as the diffusion of a short lasting [Ca^{2+}] microdomain on a very high permeability of the outer membrane.

Finally, the VDAC-dependent enhancement of mitochondrial Ca^{2+} responses potentiates the effect of apoptosis inducers, such as ceramide, in causing early alterations of organelle morphology. Interestingly, these result well correlate with those of Voehringer et al. (2000) who compared the gene expression patterns of two cells lines derived from a B cell lymphoma that differed in sensitivity to apoptosis. While antioxidant genes were highly expressed in the apoptosis-resistant cell, VDAC was shown to be strongly up-regulated upon irradiation in the apoptosis-sensitive cells. Similarly, Madesh and Hajnoczky (2001) demonstrated a key role of VDAC in activation of permeability transition pore and ensuing release of cytochrome c upon oxidative stress. Our results provide a mechanism by which the VDAC repertoire, by enhancing mitochondrial Ca^{2+} changes and Ca^{2+}-dependent changes in organelle morphology, controls the decoding of organelle Ca^{2+} signals and in particular the activation of mitochondrial apoptotic events. Interestingly, in a recent paper Csordas et al. (2002) demonstrated that a proapoptotic protein, tcBid, potentiates the transfer of IP_3-mediated Ca^{2+} signals to mitochondria. Thus, a resident ion channel, VDAC, and a proapoptotic member of the Bcl-2 family, tcBid, appear to be involved in tuning the mitochondrial Ca^{2+} signal and controlling its capacity to trigger cell death.

Much work still needs to be done for the molecular elucidation of mitochondrial Ca^{2+} homeostasis. The clarification of the important and complex role played in this process by VDAC, the most abundant channel of the outer membrane, provides a first molecular clue, thus on the one hand suggesting novel regulatory mechanisms in cellular calcium signaling and on the other identifying a potential pharmacological target in this process of major pathophysiological interest.

Materials and methods

Cell culture and transfection

Primary cultures of skeletal myotubes were prepared from newborn rats and transfected as described previously (Cantini et al., 1994). For aequorin measurements, cells (seeded onto 13-mm coverslips) were cotransfected with 3 μg mtGFP/pcDNA3 and 1 μg mtAEQmut/VR1012, mtAEQwt/pcDNA3, or erAEQmut/VR1012 (controls) or with 3 μg VDAC–GFP (VDAC inserted in pEGFP-N1 [CLONTECH Laboratories, Inc.]) and 1 μg mtAEQmut, mtAEQwt, or erAEQmut (VDAC-overexpressing). For the imaging, the cells (seeded onto 24-mm coverslips) were cotransfected with 2 μg mtBFP and 4 μg VDAC–GFP. For mitochondrial and cytosolic [Ca^{2+}] imaging, cells were cotransfected with 2 μg CaMgaroo2 and 4 μg pECFP or with 2 μg CaMgaroo2 and 4 μg VDAC–CFP (controls and VDAC-overexpressing, respectively). For the experiments in which C_2 ceramide was used, cells were transfected with 4 μg mtRFP (controls) or with 2 μg mtRFP and 4 μg VDAC–GFP (VDAC-overexpressing). In all cases, transfection was performed using the Ca^{2+}-phosphate technique. Luminescence or microscopic analyses were performed 7 d (myotubes) or 36 h (HeLa) after transfection.

Aequorin measurements

Aequorin reconstitution, luminescence measurements, and calibration into [Ca^{2+}] values were performed as described previously (Chiesa et al., 2001). In the experiments, the cells were perfused with KRB (125 mM NaCl, 5 mM KCl, 1 mM $MgSO_4$, 1 mM Na_2HPO_4, 5.5 mM glucose, 20 mM $NaHCO_3$, 2 mM L-glutamine, and 20 mM Hepes, pH 7.4, at 37°C) supplemented with either 1 mM $CaCl_2$ or 100 μM EGTA (KRB/EGTA). In the experiments with permeabilized cells, a buffer mimicking the cytosolic ionic composition, (intracellular buffer [IB]) was employed: 140 mM KCl, 10 mM NaCl, 1 mM K_3PO_4, 5.5 mM glucose, 2 mM $MgSO_4$, 1 mM ATP, 2 mM sodium succinate, and 20 mM Hepes (pH 7.05 at 37°C). IB was supplemented with either 50 μM EGTA (free [Ca^{2+}] $< 10^{-8}$ M) (IB/EGTA) or an EGTA (2 mM)-buffered [Ca^{2+}] of 1 μM (IB/1 μM Ca^{2+}), 2 μM (IB/2 μM Ca^{2+}), or 5 μM (IB/5 μM Ca^{2+}). HeLa cells were permeabilized by 1-min incubation with digitonin (added to IB/EGTA) before luminescence measurements. All of the results are expressed as means ± standard error, and Student's *t* test was used for the statistic.

Immunocytochemistry

HeLa cells (control and VDAC-overexpressing cells) were fixed in 2% paraformaldehyde for 20 min at RT. The samples were then treated for 30 min at RT with Triton 0.1% and ethanolamine 0.1 M (Sigma-Aldrich) (pH 8). The cells were incubated 2 h at RT with the anticalreticulin chicken polyclonal antibody (1:200 in BSA 3% in PBS, pH 8 [Affinity BioReagents, Inc.]) the monoclonal anti-SERCA2 ATPase (1:100; Affinity BioReagents, Inc.) or the monoclonal anti–human Glogin-97 (1:100; Molecular Probes). After three washes with PBS (10 min each), a 1-h incubation at RT with the donkey anti–chicken IgG (Cy5-conjugated, 1:200; Jackson ImmunoResearch Laboratories) or the donkey anti–mouse IgG (AlexaFluor 594, 1:200; Molecular Probes), and three washes with PBS, the samples were mounted on slides with 90% glycerol. Some other samples were incubated at 4°C overnight with the anti-Porin 31HL (VDAC) human mAb (1:100; Calbiochem). After three washes with PBS, the cells were incubated for 1 h at RT with the donkey anti–mouse IgG (AlexaFluor 594), extensively washed in PBS, and mounted with 90% glycerol. Some cells were treated only with the secondary antibodies and used to calculate values of background (due to unspecific binding) in the samples. Intensity values were calculated that eliminated 99% of the unspecific background in those cells. A threshold value for specific binding was established as the mean plus two SDs of the 99th percentile values from five cells.

Image acquisition and deconvolution

Myotubes or HeLa cells were placed in a Leyden chamber (Medical Systems Corp.) on the stage of an inverted Nikon microscope equipped with epifluorescence, piezoelectric motorization of the objective (Physik Instrumente, GmbH & Co.) and filter-wheels on the excitation and emission optical paths (Sutter Instrument Co.). Images were taken using a Nikon 60× 1.4 NA PlanAPO objective lens, a back-illuminated CCD camera (Princeton Instruments) and the Metamorph software (Universal Imaging Corp.). For computational deblurring, a stack of images was acquired through the depth of the cell and processed using the EPR software developed by the U. Mass Group (Carrington et al., 1995). For images of Figs. 1 and 10, the pixel size was 166 nm, and for Fig. 7 the pixel size was 83 nm.

Analysis of colocalization of fluorescence signals

The data analysis and visualization environment was used to visualize images in three dimensions, superimpose them, and determine the extent to which they coincided (Lifshitz et al., 1994). A custom computer program was used to first threshold each three-dimensional image in order to identify pixels belonging to mitochondria. For the images in Fig. 1, three fluorescence thresholds were chosen for each image: a low one to eliminate as much of the background fluorescence as possible while completely preserving the mitochondrial structures, a high one which completely eliminates the background and main structures begun to disappear, and a medium one by which images were processed that represented a value between the previous two. These thresholded images were then used to count total number of pixels (i.e., the total volume) occupied by the mitochondria and VDAC. Colocalization was calculated as the number of voxels (volume pixels) occupied by both signals (namely, VDAC–GFP and mtBFP) over all voxels occupied by the VDAC–GFP signal in thresholded images (Moore et al., 1993; Lifshitz et al., 1994), in other words the percentage of the overexpressed VDAC localized to mitochondria.

For the analysis of the spatial relationship among the ER, mitochondria, and VDAC, the three-dimensional images of mtBFP distribution were used to define the mitochondrial volume. The images of mtBFP, VDAC–GFP, anticalreticulin, and anti-VDAC were first thresholded to eliminate background (as described in Immunocytochemistry). The thresholded mtBFP images were used to mask the corresponding thresholded VDAC and calreticulin images sets in order to restrict the analysis of colocalization to

only those voxels corresponding to the mitochondria. The percentage of mitochondrial surface containing either VDAC–GFP, anti-VDAC, or anti-calreticulin colocalization was expressed as the number of voxels (volume pixels) occupied by either VDAC–GFP, anti-VDAC, or anticalreticulin over all voxels occupied by the mitochondrial signal mtBFP. The percentage of VDAC colocalized with calreticulin was expressed as the number of voxels occupied by both VDAC and calreticulin over all voxels occupied by the VDAC (all within the mtBFP mask).

Simultaneous measurement of mitochondrial and cytoplasmic $[Ca^{2+}]$

To monitor $[Ca^{2+}]$ in the cytosol and in mitochondria simultaneously, transfected HeLa cells were loaded with 2 μM Fura-2/AM in KRB 30 min at 37°C and 10 min at RT. Cells were then washed in the same solution, and $[Ca^{2+}]_c$ and $[Ca^{2+}]_m$ changes were determined using a high speed, wide field digital imaging microscope (ZhuGe et al., 1999 contains a complete description of this system). Briefly, the system is based on a custom built inverted microscope. An objective (Nikon 40×, 1.3 NA) forms an image on a 128 × 128 pixel (pixel size 333 nm × 333 nm) frame transfer charge-coupled device camera. Three different laser shutters controlled both the exposure time and the alternation of the three different excitation wavelengths. The sequence of excitation wavelengths was 350 and 380 nm for Fura-2/AM and 514 nm for CaMgaroo, coupled through a 525 DCXR epifluorescence dichroic. Fluorescence emission was filtered by an HQ525 long pass filter (dichroic and filter; Chroma Technology). For each sample, first a through-focus image stack for CaMgaroo (514 nm excitation) was acquired before stimulation (9 planes, 0.5 μm apart). After this, a series of 66, three wavelength image sets were acquired exposing the cell 5 ms for each wavelengths with a delay between images of 5 ms, and the acquisition was repeat every 200 ms for a total of 39.6 s After 2.4 s (12 image sets) from the beginning of the recording, cells were challenged with a 5-s puff of 10 μM histamine. For each experiment, the three-dimensional CaMgaroo stack was deconvolved using the EPR station mentioned above, an intensity threshold was chosen, and the thresholded stack was projected to form a two-dimensional mask image. This mask was used to identify mitochondrial pixels in the subsequent time series. The Fura-2/AM ratio images, corresponding to the CaMgaroo images, were calculated as 350/380. Analysis of the resulting CaMgaroo and Fura-2/AM images were performed using custom designed software running on a Silicon Graphics workstation.

Isolation of subcellular fractions and Western blot analysis

HeLa cells were plated in 10-cm Petri dishes; VDAC-overexpressing cells were transfected with 40 μg VDAC–GFP. 36 h after transfection, cells were washed twice in PBS, scraped, centrifuged (1,000 rpm, 5 min, 25°C), and resuspended in 4 ml of buffer A (10 mM NaCl, 10 mM Tris-HCl, pH 7.4, 1.5 mM $CaCl_2$). All of the following steps were performed at 4°C. Cells were homogenized in Glas-Glas homogenier and 2 ml of buffer B (0.75 M sucrose, 60 mM Tris-HCl, pH 7.4, 3 mM EDTA, 3 mM EGTA, 3 mM $MgCl_2$, 3 mM PMSF, protease inhibitor cocktail [P-8340; Sigma-Aldrich], 3mM DTT) were immediately added. Homogenates were centrifuged at 510 *g* for 10 min, and then the supernatants were recentrifuged at the same speed. Mitochondria were pelleted by centrifugation at 9,000 *g* for 10 min, resuspended in buffer C (0.25 M sucrose, 20 mM Tris-HCl, pH 7.4, 1 mM EDTA, 1 mM EGTA, 1 mM $MgCl_2$, 1 mM PMSF, protease inhibitor cocktail, 1 mM DTT), centrifuged again in order to eliminate microsomal and cytosolic contamination, and resuspended in 200 μl of buffer C. The post-mitochondrial supernatants were centrifuged at 15,000 *g* for 30 min in order to remove lysosomal fraction. To separate cytosolic and microsomal fraction, the final supernatants were filtered through a 0.2 μm (Schleicher & Schuell GmbH) filter. Protein determination was performed according to the Bradford method. The proteins were separated by SDS-PAGE on 14% gel, and the amount of endogenous VDAC, VDAC–GFP, and Bax, and the marker proteins SERCA and β-tubulin was estimated by Western blotting using rabbit anti-VDAC (1:5,000; a gift from Dr. V. De Pinto, University of Catania, Catania, Italy) and anti-Bax (1:10,000; Santa Cruz Biotechnology) polyclonal antibodies and mouse anti–β-tubulin (1:5,000; Santa Cruz Biotechnology) and anti-SERCA2 (Affinity BioReagents) mAbs revealed with and anti–rabbit and mouse IgG HRP-labeled secondary antibodies (1:10,000; Santa Cruz Biotechnology), respectively, according to standard protocols. Proteins were visualized by ECL (Amersham Biosciences).

We thank Drs. Shoshan-Barmatz (Ben Gurion University, Be'er Sheva, Israel) and Herman (University of Texas Health Science Center, San Antonio, TX) for providing the VDAC–GFP cDNA, Dr. Tsien for critically reading the manuscript, and Drs. Brini, Walsh, and Pozzan for helpful discussions.

We thank Telethon-Italy (grant nos. 1285 and GTF01011), the Italian Association for Cancer Research, the Human Frontier Science Program, the Italian University Ministry, the Italian Space Agency, the National Research Council, the National Institutes of Health (HL 61297 and GM 61981), and the National Science Foundation (DBI 9724611 and DIR 9200027) for financial support. E. Rapizzi, M.R. Wiechowski, and G. Vandecasteele are recipients of Telethon, the Federation of European Biochemical Societies, and European Molecular Biology Organization long term fellowships, respectively. This research has been supported by a Marie Curie Fellowship (contract no. HPMF-CT-2000-00644).

Submitted: 17 May 2002
Revised: 1 October 2002
Accepted: 1 October 2002

References

Babcock, D.F., J. Herrington, P.C. Goodwin, Y.B. Park, and B. Hille. 1997. Mitochondrial participation in the intracellular Ca^{2+} network. *J. Cell Biol.* 136:833–843.

Baird, G.S., D.A. Zacharias, and R.Y. Tsien. 1999. Circular permutation and receptor insertion within green fluorescent proteins. *Proc. Natl. Acad. Sci. USA.* 96:11241–11246.

Barrero, M.J., M. Montero, and J. Alvarez. 1997. Dynamics of $[Ca^{2+}]$ in the endoplasmic reticulum and cytoplasm of intact HeLa cells: a comparative study. *J. Biol. Chem.* 272:27694–27699.

Boitier, E., R. Rea, and M.R. Duchen. 1999. Mitochondria exert a negative feedback on the propagation of intracellular Ca^{2+} waves in rat cortical astrocytes. *J. Cell Biol.* 145:795–808.

Brini, M., F. De Giorgi, M. Murgia, R. Marsault, M.L. Massimino, M. Cantini, R. Rizzuto, and T. Pozzan. 1997. Subcellular analysis of Ca^{2+} homeostasis in primary cultures of skeletal muscle myotubes. *Mol. Biol. Cell.* 8:129–143.

Cantini, M., M.L. Massimino, C. Catani, R. Rizzuto, M. Brini, and U. Carraro. 1994. Gene transfer into satellite cell from regenerating muscle: bupivacaine allows beta-Gal transfection and expression in vitro and in vivo. *In Vitro Cell. Dev. Biol. Anim.* 30:131–133.

Carrington, W.A., R.M. Lynch, E.D. Moore, G. Isenberg, K.E. Fogarty, and F.S. Fay. 1995. Superresolution three-dimensional images of fluorescence in cells with minimal light exposure. *Science.* 268:1483–1487.

Chiesa, A., E. Rapizzi, V. Tosello, P. Pinton, M. De Virgilio, K.E. Fogarty, and R. Rizzuto. 2001. Recombinant aequorin and green fluorescent protein as valuable tools in the study of cell signalling. *Biochem. J.* 355:1–12.

Colombini, M. 1979. A candidate for the permeability pathway of the outer mitochondrial membrane. *Nature.* 279:643–645.

Crompton, M. 2000. Mitochondria intermembrane junctional complexes and their role in cell death. *J. Physiol.* 529:11–21.

Csordas, G., A.P. Thomas, and G. Hajnoczky. 1999. Quasi-synaptic calcium signal transmission between endoplasmic reticulum and mitochondria. *EMBO J.* 18:96–108.

Csordas, G., M. Madesh, B. Antonsson, and G. Hajnoczky. 2002. tcBid promotes Ca(2+) signal propagation to the mitochondria: control of Ca(2+) permeation through the outer mitochondrial membrane. *EMBO J.* 21:2198–2206.

Drummond, R.M., T.C. Mix, R.A. Tuft, J.V. Walsh, Jr., and F.S. Fay. 2000. Mitochondrial Ca2+ homeostasis during Ca2+ influx and Ca2+ release in gastric myocytes from Bufo marinus. *J. Physiol.* 522:375–390.

Duchen, M.R. 2000. Mitochondria and calcium: from cell signalling to cell death. *J. Physiol.* 529:57–68.

Gerencser, A.A., and V. Adam-Vizi. 2001. Selective, high-resolution fluorescence imaging of mitochondrial Ca^{2+} concentration. *Cell Calcium.* 30:311–321.

Gincel, D., H. Zaid, and V. Shoshan-Barmatz. 2001. Calcium binding and translocation by the voltage-dependent anion channel: a possible regulatory mechanism in mitochondrial function. *Biochem. J.* 358:147–155.

Griesbeck, O., G.S. Baird, R.E. Campbell, D.A. Zacharias, and R.Y. Tsien. 2001. Reducing the environmental sensitivity of yellow fluorescent protein. Mechanism and applications. *J. Biol. Chem.* 276: 29188–29194.

Hajnoczky, G., L.D. Robb-Gaspers, M.B. Seitz, and A.P. Thomas. 1995. Decoding of cytosolic calcium oscillations in the mitochondria. *Cell.* 82:415–424.

Hajnoczky, G., R. Hager, and A.P. Thomas. 1999. Mitochondria suppress local feedback activation of inositol 1,4,5-trisphosphate receptors by Ca^{2+}. *J. Biol. Chem.* 274:14157–14162.

Jouaville, L.S., P. Pinton, C. Bastianutto, G.A. Rutter, and R. Rizzuto. 1999. Regulation of mitochondrial ATP synthesis by calcium: evidence for a long-term metabolic priming. *Proc. Natl. Acad. Sci. USA.* 96:13807–13812.

Landolfi, B., S. Curci, L. Debellis, T. Pozzan, and A.M. Hofer. 1998. Ca^{2+} homeostasis in the agonist-sensitive internal store: functional interactions between mitochondria and the ER measured In situ in intact cells. *J. Cell Biol.* 142:1235–1243.

Lee, A.C., X. Xu, and M. Colombini. 1996. The role of pyridine dinucleotides in regulating the permeability of the mitochondrial outer membrane. *J. Biol. Chem.* 271:26724–26731.

Lifshitz, L., E. Collins, G. Moore, and J. Gauch. 1994. Computer vision and graphics in fluorescence microscopy. *In* Proceedings of the Biomedical Imaging Workshop. Institute of Electrical and Electronic Engineers. Computer Soc. Press, Los Angeles, CA. 166–175.

Madesh, M., and G. Hajnoczky. 2001. VDAC-dependent permeabilization of the outer mitochondrial membrane by superoxide induces rapid and massive cytochrome c release. *J. Cell Biol.* 155:1003–1015.

Mannella, C.A. 1998. Conformational changes in the mitochondrial channel protein, VDAC, and their functional implications. *J. Struct. Biol.* 121:207–218.

McCormack, J.G., A.P. Halestrap, and R.M. Denton. 1990. Role of calcium ions in regulation of mammalian intramitochondrial metabolism. *Physiol. Rev.* 70:391–425.

Montero, M., M.T. Alonso, E. Carnicero, I. Cuchillo-Ibanez, A. Albillos, A.G. Garcia, J. Garcia-Sancho, and J. Alvarez. 2000. Chromaffin-cell stimulation triggers fast millimolar mitochondrial Ca^{2+} transients that modulate secretion. *Nat. Cell Biol.* 2:57–61.

Moore, E.D., E.F. Etter, K.D. Philipson, W.A. Carrington, K.E. Fogarty, L.M. Lifshitz, and F.S. Fay. 1993. Coupling of the Na+/Ca2+ exchanger, Na+/K+ pump and sarcoplasmic reticulum in smooth muscle. *Nature.* 365:657–660.

Pinton, P., D. Ferrari, E. Rapizzi, F. Di Virgilio, T. Pozzan, and R. Rizzuto. 2001. The Ca^{2+} concentration of the endoplasmic reticulum is a key determinant of ceramide-induced apoptosis: significance for the molecular mechanism of Bcl-2 action. *EMBO J.* 20:2690–2701.

Rizzuto, R., M. Brini, M. Murgia, and T. Pozzan. 1993. Microdomains with high Ca^{2+} close to IP3-sensitive channels that are sensed by neighboring mitochondria. *Science.* 262:744–777.

Rizzuto, R., P. Pinton, W. Carrington, F.S. Fay, K.E. Fogarty, L.M. Lifshitz, R.A. Tuft, and T. Pozzan. 1998. Close contacts with the endoplasmic reticulum as determinants of mitochondrial Ca^{2+} responses. *Science.* 280:1763–1766.

Rizzuto, R., P. Bernardi, and T. Pozzan. 2000. Mitochondria as all-round players of the calcium game. *J. Physiol.* 529:37–47.

Robb-Gaspers, L.D., P. Burnett, G.A. Rutter, R.M. Denton, R. Rizzuto, and A.P. Thomas. 1998. Integrating cytosolic calcium signals into mitochondrial metabolic responses. *EMBO J.* 17:4987–5000.

Rostovtseva, T., and M. Colombini. 1996. ATP flux is controlled by a voltage-gated channel from the mitochondrial outer membrane. *J. Biol. Chem.* 271: 28006–28008.

Sampson, M.J., L. Ross, W.K. Decker, and W.J. Craigen. 1998. A novel isoform of the mitochondrial outer membrane protein VDAC3 via alternative splicing of a 3-base exon. *J. Biol. Chem.* 273:30482–30486.

Shoshan-Barmatz, V., N. Hadad, W. Feng, I. Shafir, I. Orr, M. Varsanyi, and L.M. Heilmeyer. 1996. VDAC/porin is present in sarcoplasmic reticulum from skeletal muscle. *FEBS Lett.* 386:205–210.

Tinel, H., J.M. Cancela, H. Mogami, J.V. Gerasimenko, O.V. Gerasimenko, A.V. Tepikin, and O.H. Petersen. 1999. Active mitochondria surrounding the pancreatic acinar granule region prevent spreading of inositol trisphosphate-evoked local cytosolic Ca^{2+} signals. *EMBO J.* 18:4999–5008.

Vander Heiden, M.G., X.X. Li, E. Gottleib, R.B. Hill, C.B. Thompson, and M. Colombini. 2001. Bcl-xL promotes the open configuration of the voltage-dependent anion channel and metabolite passage through the outer mitochondrial membrane. *J. Biol. Chem.* 276:19414–19419.

Voehringer, D.W., D.L. Hirschberg, J. Xiao, Q. Lu, M. Roederer, C.B. Lock, L.A. Herzenberg, L. Steinman, and L.A. Herzenberg. 2000. Gene microarray identification of redox and mitochondrial elements that control resistance or sensitivity to apoptosis. *Proc. Natl. Acad. Sci. USA.* 97:2680–2685.

ZhuGe, R., R.A. Tuft, K.E. Fogarty, K. Bellve, F.S. Fay, and J.V. Walsh, Jr. 1999. The influence of sarcoplasmic reticulum Ca2+ concentration on Ca2+ sparks and spontaneous transient outward currents in single smooth muscle cells. *J. Gen. Physiol.* 113:215–228.